Unsupervised Detection of Active, New, and Closed Coal Mines with Reclamation Activity from Landsat 8 OLI/TIRS Images

Jit Mukherjee[1(✉)], Jayanta Mukherjee[2], Debashish Chakravarty[3], and Subhas Aikat[2]

[1] Advance Technology Development Centre, Indian Institute of Technology, Kharagpur, Kharagpur, West Bengal, India
jit.mukherjee@iitkgp.ac.in

[2] Department of Computer Science and Engineering, Indian Institute of Technology, Kharagpur, Kharagpur, West Bengal, India
jay@cse.iitkgp.ac.in, subhas.aikat@iitkgp.ac.in

[3] Department of Mining Engineering, Indian Institute of Technology, Kharagpur, Kharagpur, West Bengal, India
dc@mining.iitkgp.ernet.in

Abstract. Monitoring and classification of surface coal mine regions have several research aspects, as they have huge impacts on the eco-environment of a region. Mining regions change over time immensely. New potential mines get opened. Whereas, few mines stay active and many of them get closed. Closed mine regions are reclaimed to environment through plantation. In the past, semi-supervised and supervised techniques have been used to detect mine classes and assess the changes of land use and land cover classes. In this work, mine regions are detected in an adaptive manner from satellite images unlike the techniques in the literature. Further, a change detection technique is used to detect active, new, and closed surface coal mines in a region. Detected closed mines are further analysed to evaluate reclamation of that region. Average precision and recall of active, new, and closed mining regions of the proposed technique are found to be $[84.7\%, 62.8\%]$, $[74.2\%, 64.5\%]$, and $[70.1\%, 58.2\%]$, respectively.

Keywords: Clay mineral ratio · Coal mine index · Surface coal mine · Change detection · Mine classes · Landsat 8

1 Introduction

Surface mining is a widely used mining technique, and has several advantages. It creates irreversible damage to the ecosystem, serious land degradation, loss of vegetation, contamination, etc. [4,7]. Large scale surface mining directly impacts soil fertility, desertification factors, biodiversity, etc. [4,8]. Coal surface mining

has severe environmental adversities because of coal seam fires. In surface mining, a shallow ore deposit is extracted by removing the overlaying soil and creating a pit. Extracted minerals and waste materials are dumped in nearby regions. Such land use and land cover changes due to mining show the paramount correlation of human activities to environment [13]. Therefore, quantification of land use and land cover changes in mining regions have several impacts and various research challenges. Detection and classification of surface mining regions have various research aspects such as mine waste water detection and treatment [9,11], assessment of reclamation success [13,14], detection of surface mining land classes [13], coal seam fire detection and management [6], etc. Supervised support vector machine based classification has been used in [13] to detect changes due to surface mining and reclamation in the island of Milos in Greece and to detect various land classes and to quantify reclamation success [7]. In [4], various vegetation indexes are considered to detect mine wasteland. Vegetation recovery on reclaimed coal surface mining areas has been measured through field validation in south western Virginia, USA [5]. In [3], two different classification approaches are used to detect coal surface mine land cover classes such as object and spectral based approaches. Most of these works detect several land classes in mine region through supervised and semi-supervised techniques and subsequently use these land classes to assess reclamation success through change detection. Clay mineral ratio detects the volume of hydrothermally altered rock in clay [2]. It has been found resourceful to detect various surface mine land classes in adaptive fashion [9,11]. In [10], coal mine regions are detected using a spectral index over *SWIR-I* and *SWIR-II* bands, called coal mine index (*CMI*). Further, it is also used to detect coal mine regions adaptively through hierarchical K-Means clustering [12]. In this work, the concept presented in [12] has been used to detect coal mine regions over multi-temporal Landsat images. These regions are further analyzed to check whether they are active, closed or newly created. The closed down mines are further checked whether they are reclaimed.
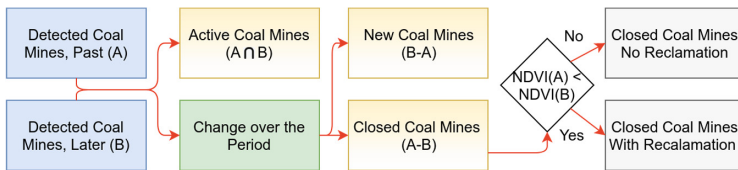

Fig. 1. Flow diagram of the proposed technique

2   Methodology

In this work, Landsat 8 multi-temporal images are used. The flow diagram of the proposed method is shown in Fig. 1. As shown in Fig. 1(A) and (B), coal

mine regions are detected in unsupervised fashion from Landsat 8 images, where acquisition time of A is before the acquisition time of B. These images are further analysed by a change detection technique. It produces two images showing the unchanged and the changed regions, where land cover changes have occurred. The latter image is further analysed to detect the closed and new coal mines. Thereafter, Normalized difference vegetation index ($NDVI$) values are examined over the closed mine regions to detect reclamation regions.

2.1   Adaptive Detection of Coal Mine Regions

A spectral index, namely coal mine index (CMI), has been proposed as $\phi(SWIR-I, SWIR-II)$, i.e. $\frac{\lambda_{SWIR-I} - \lambda_{SWIR-II}}{\lambda_{SWIR-I} + \lambda_{SWIR-II}}$, where λ_{SWIR-I}, and $\lambda_{SWIR-II}$ represent reflectance values in short wave infra-red one, and short wave infra-red two band, respectively [10]. It is detected as a coal mine region if $\phi(SWIR-I, SWIR-II) < \tau$ [10], where τ is an empirical threshold. In [12], a novel method has been proposed to detect coal mine regions in an adaptive manner using CMI. It has been found that lower values of CMI have higher probability of being a coal mine region [10,12]. In [12], CMI values are hierarchically clustered using K-Means Clustering, where $k = 2$. The cluster associated with the higher CMI values is discarded, and that with lower CMI values is preserved. The process is repeated at a number of levels of hierarchy. It has been found that coal mine regions are detected at level three for Jharia coal mine region [12]. In this work, the proposed method uses the technique in [12] to detect active, new and closed mine using temporal analysis.

2.2   Adaptive Detection of Active, New and Closed Coal Mines with Reclamation

Active, new, and closed coal mine regions are detected using change detection technique. Let, A, and B be the detected coal mining regions of the same geographical region over a period, where acquisition time of A is before the acquisition time of B. A, and B have several regions in common. These regions are detected as active mine regions ($ActiveMines = A \cap B$). Mines, which are detected in A but not in B, are denoted as closed mines ($ClosedMines = A - B$). Whereas, mines, which are detected in B but not in A, are denoted as new mines ($NewMines = B - A$).

Further, reclamation impacts are computed in closed mine regions. In reclamation, trees are planted in a closed mine area to control its impact on environment. Therefore, vegetation index values of the closed mines are further analysed. Here, the $NDVI$ is used to compute the vegetation values. It is denoted by $\phi(NIR, Red)$ [4]. Here, Red, and NIR are the reflectance values of Red and Near Infra-red bands. Higher values of $NDVI$ denote vegetation in a region [15]. A closed mine is detected as reclamation region if $NDVI(A) < NDVI(B)$. Otherwise, the regions are denoted as closed coal mine regions without reclamation. The proposed method is applicable for multispectral remote sensing images with Red, NIR, $SWIR$-I, and $SWIR$-II bands.

3   Data and Study Area

In this work radiometrically corrected, geo-referenced, multi-temporal Landsat 8 $L1$ images are used over the Jharia Coal Field (JCF) regions from $USGS$ archive. It has an additional criteria of $< 10\%$ cloud cover. The JCF region is situated in the Gondwana basin of the Damodar valley in the state of Jharkhand, India ranging between $23°38'$ N and $23°50'$ N and longitudes $86°07'E$ and $86°30'E$. The JCF is a sickle shaped coal field, which resides among other prominent coal fields of Raniganj, Bokaro, Karanpura, Ramgarh and Hutar in the eastern part of Damodar valley. It has diverse range of land cover classes such as mine regions, dense forest, urban settlement, fresh water bodies, rivers, river bed, grassland, dry crop lands, etc. Landsat 8 provides nine multi-spectral and two thermal image bands with the temporal resolution of 16 days. They have spatial resolution of 30 meter except the panchromatic band. $L1$ data products provide top of atmosphere (TOA) reflectance values. In this work, Landsat images of 2013, and 2018 have been used for experimentation. High resolution Google Earth™ historical images of this period are obtained for ground truth generation. In this work, coal quarry and coal dump regions are treated as target locations. These regions are marked from historical and recent Google Earth™ images through visual inspection and experts' opinion. Further, active, new, and closed mine locations are also marked for validation of the proposed technique.

4   Results

In this work, TOA reflectance values are computed from multi-temporal Landsat 8 images as per [1] to detect active, new, closed coal surface mines of a region. The proposed technique has a pipeline of processes. First, coal mine regions are detected from Landsat 8 $L1$ images in 2013, and 2018. The coal mine regions are detected by an adaptive technique using CMI [10], as described in Sect. 2.1. It has been found that CMI can significantly differentiate coal mine regions from other land classes. The manual thresholding technique over CMI
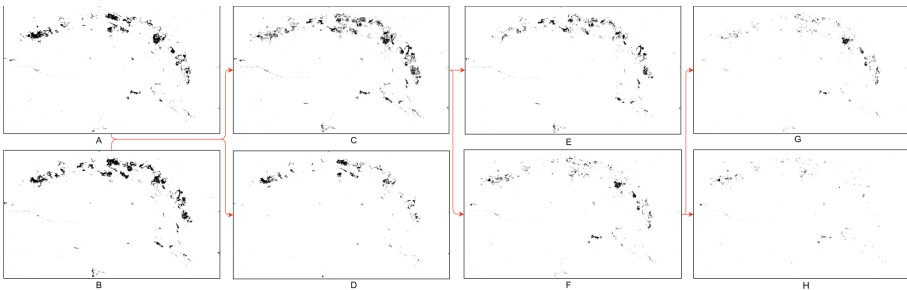

Fig. 2. A. Detected mines in 2013, B. Detected mines in 2018, C. Change in mine locations during 2013–2018, D. Active mines, E. New mines in 2018, F. Closed mines in 2018, G. Closed mines without reclamation, H. Reclaimed closed mines.
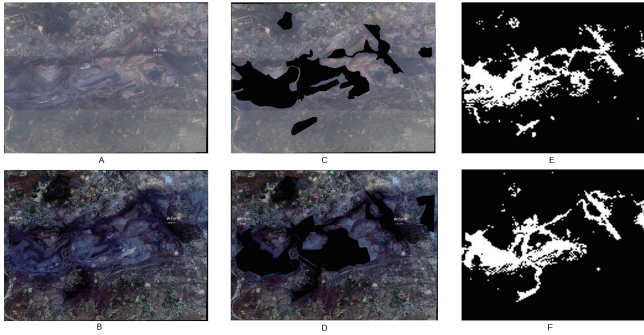
Fig. 3. (A) Google earth™ image in 2013, (B) Google earth™ image in 2018, (C) Marked mining region of (A) in black, (D) Marked mining region of (B) in black, (E) Detected mining region in 2013, (F) Detected mining region in 2018.
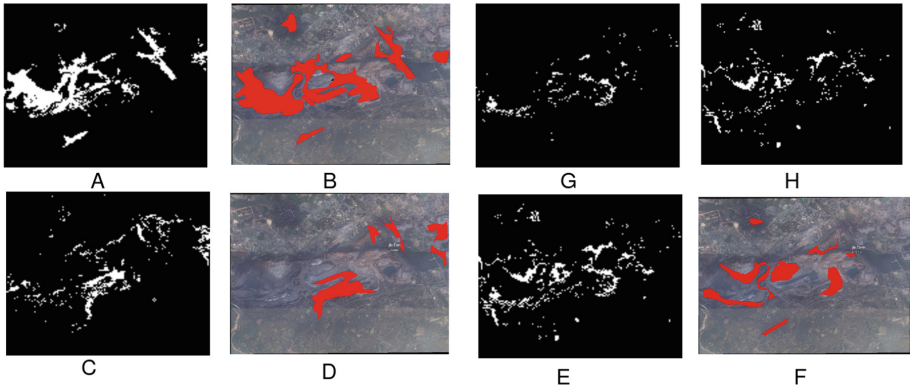

Fig. 4. (A) Active mines (B) Ground truth active mines marked in red (C) New mines (D) Ground truth new mines in red (E) Closed mines (F) Ground truth closed mines in red (G) Non-reclaimed closed mine (H) Reclaimed closed mines.

provides average accuracy[1] of 86.24% [10]. The automated detection of coal mine region has average precision, and recall of 76.43%, and 62.75%, respectively [12]. Detected coal mine regions of *JCF* in 2013, and 2018 are shown in Fig. 2(A) and (B), respectively. The black pixels in Fig. 2(A)–(H) shows various detected land cover classes of mining regions. Next, these two images with detected coal mine regions are further analysed to detect the changes of land cover and land use over the period as discussed in Sect. 2.2. Coal mine regions, which remain unchanged during this period, are treated as the active mine regions as shown in Fig. 2(D). Figure 2(C) shows the land use changes in mine regions from 2013

---

[1] Precision, Recall, and Accuracy are defined as $t_p/(t_p + f_p)$, $t_p/(t_p+f_n)$, and $(t_p + t_n)/(t_p + t_n + f_p + f_n)$, where t_p, f_p, f_n, and t_n are true positive, false positive, false negative, and true negative, respectively.

to 2018. Figure 2(C) is composed of various sub classes such as, new mines, closed mines, which are reclaimed, and closed mines, which are not reclaimed. Next, Fig. 2(C) is further analysed to detect these sub classes. Regions, which are detected as non mine land classes in Fig. 2(A) but detected as mining regions in Fig. 2(B), are marked as new mining regions. It is shown in Fig. 2(E). Detected closed down mine regions are shown in Fig. 2(F). These closed mines may have reclaimed to the environment. Hence, it is further analysed by the change of *NDVI* values in these regions. If the *NDVI* values are found to be greater than previous image, the regions is considered to be in the process of reclamation, as shown in Fig. 2(H). Otherwise, the regions are considered to be not in the process of reclamation as shown in Fig. 2(G). Figure 2 shows result over the whole Jharia region. For better understanding, results of an area of interest with ground truth images in 2013 and 2018 are shown in Fig. 3. The black portion of Fig. 3(C) and (D) represent the ground truth surface mining region in 2013, and 2018 images, respectively. It can be observed from ground truth and output images in Fig. 3 that mine regions have been changed significantly between 2013 and 2018. Further, the changes of the mining regions are computed. Let, A, and B be the processed images from 2013, and 2018, respectively. The proposed technique computes three images, such as active mines ($A \cap B$), new mines ($B - A$), and closed mines ($A - B$). Ground truths are generated over these three land classes as shown in Fig. 4. Detected active mining regions, and ground truth active mining regions are shown in Fig. 4(A) and (B), respectively. It is observed from these two images that the proposed technique detects many of the active mining regions. The precision, and recall of detection of active mining regions are found to be 84.7%, and 62.8%, respectively as shown in Table 1 (Right). Detected new mining regions, and marked ground truth image are shown in Fig. 4(C) and (D), respectively. It can be found that most of the detected new mining regions are similar with the ground truth new mining regions. Whereas, Fig. 4(C) also falsely detect some regions as new mining regions. The precision, and recall of new mining regions are found to be 74.2%, and 64.5, respectively. Similarly, detected, and ground truth closed mines are shown in Fig. 4(E) and (F), respectively. Precision, and recall of closed mining regions are found as 70.1%, and 58.2%, respectively. Precision and recall of closed and new mining regions are less than active mining land classes. The perimeter of a mining region changes over time. The walls of the mining pits are detected as mining region by the technique discussed in [10,12]. It is observed from Fig. 4(E), some of the detected regions are the walls of the mining pit. These affect the accuracy of the proposed technique. In the past, supervised and semi-supervised techniques are used to detect such mine land classes. In [7], a supervised support vector machine has been used in multi-temporal Landsat images to classify various land cover classes with average accuracy of 89.4%, and 96% in Landsat 5, and 8 images, respectively. Thereafter, reclamation is analyzed over these land classes. In [16], land reclamation monitoring has been done using pixel and object based classification in ArcGIS 9.0 platform. It has been found that 52% of closed mining areas are reclaimed, whereas field study shows 79% areas are reclaimed [16].

In [13], various land cover classes in mining region are classified using supervised support vector machine with average accuracy of 94% to detect land cover changes. The proposed method, though providing a lower accuracy, is an unsupervised technique to detect such land classes, and does not require labeled data set. Further, closed mining regions are analyzed for reclamation. Closed mining regions without reclamation and with reclamation are shown in Fig. 4(G) and (H), respectively. The *NDVI* detects the portion of vegetation in a region. In reclamation, mining regions are taken back to environment through plantation. Therefore, *NDVI* is used here to separate closed mining region with reclamation from other mine land classes. It has been observed that most of the regions, which are detected as possible reclamation regions in Fig. 4(H), have visible vegetation in the ground truth images. Further, for validation, t-test has been performed over the null hypothesis $\mu_{Reclamation} = \mu_{mlc}$, where $\mu_{Reclamation}$, and μ_{mlc}, represent mean of ground truth reclamation areas, and mean of other mine land cover classes, respectively. Here, ground truth coal quarry, coal dump, mine water bodies, and coal overburden areas are considered as other mine land cover classes. $S_{Reclamation} \neq S_{mlc}$ is considered here, where $S_{Reclamation}$, and S_{mlc} represent variance of ground truth reclamation regions, and other mine land classes, respectively. t-test result with null, and alternative hypothesis as $\mu_{Reclamation} = \mu_{mlc}$, and $\mu_{Reclamation} \neq \mu_{mlc}$, respectively, are shown in Table 1 (Left). As shown in Table 1 (Left), the null hypothesis is rejected. Therefore, the *NDVI* can distinguish reclamation regions from other mine land classes. Another advantage of the proposed technique is that use of CMI makes it applicable over the season [10, 12].

Table 1. (Left) T test results with mine reclamation regions and other mine land classes. (Right) Precision and recall of various mine land classes

T test results					Accuracy computation			
	Dump	Quarry	Overburden	Mine swamp		New	Active	Closed
t_0	7.46	8.74	3.15	12.99	Precision	74.2	84.7	70.1
df	180.5	183.1	183.2	99	Recall	61.5	62.8	58.2
P value	<0.00001	<0.00001	0.0019	<0.00001	F_1 score	67.25	72.12	63.59

5   Conclusion

In this work, an unsupervised method has been proposed to detect active, new, and closed coal mine regions in an adaptive manner. First, coal mine regions are detected without supervision using *CMI*. A change detection technique during 2013–2018 is used over to detect the mentioned land classes. Closed mining regions are further analyzed to detect reclamation regions. In the past, semi-supervised and supervised techniques have been used to detect such

classes. The proposed method has average precision and recall of [84.7%, 62.8%], [74.2%, 64.5%], and [70.1%, 58.2%], for active, new and closed mining regions, respectively. Changes of perimeter of the pit walls are detected by the proposed technique as closed or new mining regions, which affects the accuracy. Further experimentation in this regard is considered as a future direction. The method detects only those reclamation regions which are effective in this period.

References

1. Using the usgs landsat8 product. https://landsat.usgs.gov/using-usgs-landsat-8-product. Accessed 29 03 2018
2. Drury, S.A.: Image Interpretation in Geology. No. 551.0285 D796 1993, Chapman and Hall, London (1993)
3. Gao, Y., Kerle, N., Mas, J.F.: Object-based image analysis for coal fire-related land cover mapping in coal mining areas. Geocarto Int. **24**(1), 25–36 (2009)
4. Han, Y., Li, M., Li, D.: Vegetation index analysis of multi-source remote sensing data in coal mine wasteland. New Zealand J. Agric. Res. **50**(5), 1243–1248 (2007)
5. Holl, K.D.: Long-term vegetation recovery on reclaimed coal surface mines in the eastern USA. J. Appl. Ecol. **39**(6), 960–970 (2002)
6. Huo, H., et al.: A study of coal fire propagation with remotely sensed thermal infrared data. Rem. Sens. **7**(3), 3088–3113 (2015)
7. Karan, S.K., Samadder, S.R., Maiti, S.K.: Assessment of the capability of remote sensing and gis techniques for monitoring reclamation success in coal mine degraded lands. J. Environ. Manag. **182**, 272–283 (2016)
8. Lima, A.T., Mitchell, K., O'Connell, D.W., Verhoeven, J., Van Cappellen, P.: The legacy of surface mining: remediation, restoration, reclamation and rehabilitation. Environ. Sci. Pol. **66**, 227–233 (2016)
9. Mukherjee, J., Mukherjee, J., Chakravarty, D.: Automated seasonal separation of mine and non mine water bodies from landsat 8 OLI/TIRS using clay mineral and iron oxide ratio. IEEE JSTARS **12**(7), 2550–2556 (2019)
10. Mukherjee, J., Mukherjee, J., Chakravarty, D., Aikat, S.: A novel index to detect opencast coal mine areas from landsat 8 OLI/TIRS. IEEE JSTARS **12**(3), 891–897 (2019)
11. Mukherjee, J., Mukhopadhyay, J., Chakravarty, D.: Investigation of seasonal separation in mine and non mine water bodies using local feature analysis of landsat 8 OLI/TIRS images. In: IEEE IGARSS 2018, Valencia, Spain, 22–27 July 2018, pp. 8961–8964 (2018)
12. Mukherjee, J., Mukhopadhyay, J., Chakravarty, D., Aikat, S.: Automated seasonal detection of coal surface mine regions from landsat 8 oli images. In: IEEE IGARSS 2019, Yokoham, Japan, 27 July–3 August 2019 (2019)
13. Petropoulos, G.P., Partsinevelos, P., Mitraka, Z.: Change detection of surface mining activity and reclamation based on a machine learning approach of multi-temporal landsat TM imagery. Geocarto Int. **28**(4), 323–342 (2013)
14. Raval, S., Merton, R., Laurence, D.: Satellite based mine rehabilitation monitoring using worldview-2 imagery. Min. Technol. **122**(4), 200–207 (2013)
15. Silleos, N.G., Alexandridis, T.K., Gitas, I.Z., Perakis, K.: Vegetation indices: advances made in biomass estimation and vegetation monitoring in the last 30 years. Geocarto Int. **21**(4), 21–28 (2006)
16. Singh, N., Gupta, V., Singh, A.: Geospatial technology for land reclamation monitoring of open cast coal mines in India. In: Proceedings of ISPRS, pp. 1–4 (2011)